Chemical Engineering Journal 338 (2018) 323–332

Contents lists available at ScienceDirect

Chemical Engineering Journal

journal homepage: www.elsevier.com/locate/cej

Hydrodynamic cavitation and activated persulfate oxidation for degradation of bisphenol A: Kinetics and mechanism

Jongbok Choi[a], Mingcan Cui[a], Yonghyeon Lee[a], Jeonggwan Kim[b], Younggyu Son[c], Jeehyeong Khim[a,*]

[a] School of Civil, Environmental, and Architectural Engineering, Korea University, 145 Anam-ro, Seongbuk-gu, Seoul 02841, Republic of Korea
[b] Korea Environmental Industry and Technology, Seoul 03367, Republic of Korea
[c] Department of Civil, Environmental and Environmental Engineering, Kumoh National Institute of Technology, Daehak-ro 61, Gumi, Gyeongbuk 730-701, Republic of Korea

HIGHLIGHTS

- A new oxidation mechanism for BPA is proposed.
- The respective contributions of ·OH (10.32%) and SO_4^{-}· (89.68% for BPA removal were determined.
- Cl anions affected HC/PS systems removal of BPA.
- Economics of HC/PS systems were based on energy and oxidant consumption.

GRAPHICAL ABSTRACT

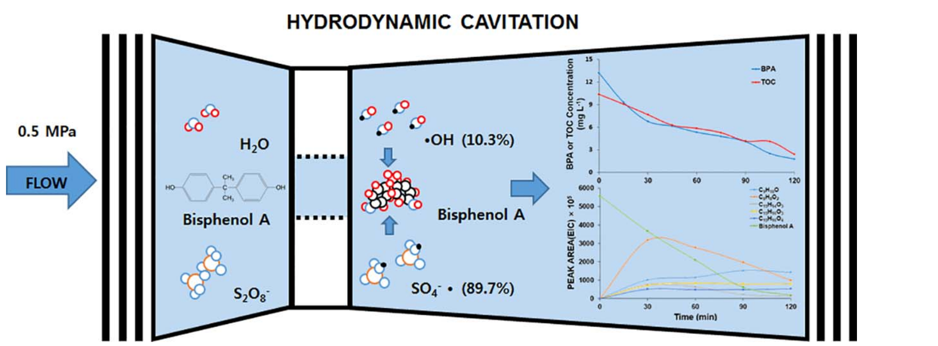

ARTICLE INFO

Keywords:
Hydrodynamic cavitation/persulfate process
Sulfate radical
Hydroxyl radical
Bisphenol A
Activation energy
Mechanism

ABSTRACT

Bisphenol A (BPA) is an endocrine disruptor and is toxic at low concentrations. Furthermore, in order to oxidize BPA at the water treatment, an economical treatment method is required. This study was the first study to apply hydrodynamic cavitation/persulfate (HC/PS) processes to degrade BPA and investigated the effects of important operating parameters, such as HC inlet pressure, PS loading, pH, temperature and other anions. The results showed that the optimal pressure of HC was 0.5 MPa and the rate constant increased as the PS load concentration increased. The contribution of ·OH and $SO_4^{-\cdot}$ to BPA oxidation using HC/PS processes was 10.3% and 89.7%, respectively. The reaction rate constant decreased with increasing pH and the reaction rate constant increased with increasing temperature. The activation energy was 69.62 kJ mol^{-1}. The effects of other anions on BPA degradation were in the following order: $Cl^{-} > NO_3^{-} > HCO_3^{-}$. Five major intermediates were formed in the HC/PS processes and they were obtained during 120 min of operation. Based on this, this study described the decomposition pathway of BPA. The kinetic study and economic evaluation of the HC/PS processes can be used as basic data for the real wastewater treatment process in the future.

1. Introduction

Bisphenol A (BPA) is one of the most representative members of the endocrine disrupting chemicals (EDCs) family, and this is mainly owing to its excessive use. Specifically, BPA is known to exhibit weak estrogenic activity at concentrations that can correspond to an extremely

* Corresponding author.
E-mail address: hyeong@korea.ac.kr (J. Khim).

https://doi.org/10.1016/j.cej.2018.01.018
Received 18 October 2017; Received in revised form 11 December 2017; Accepted 2 January 2018
Available online 06 January 2018

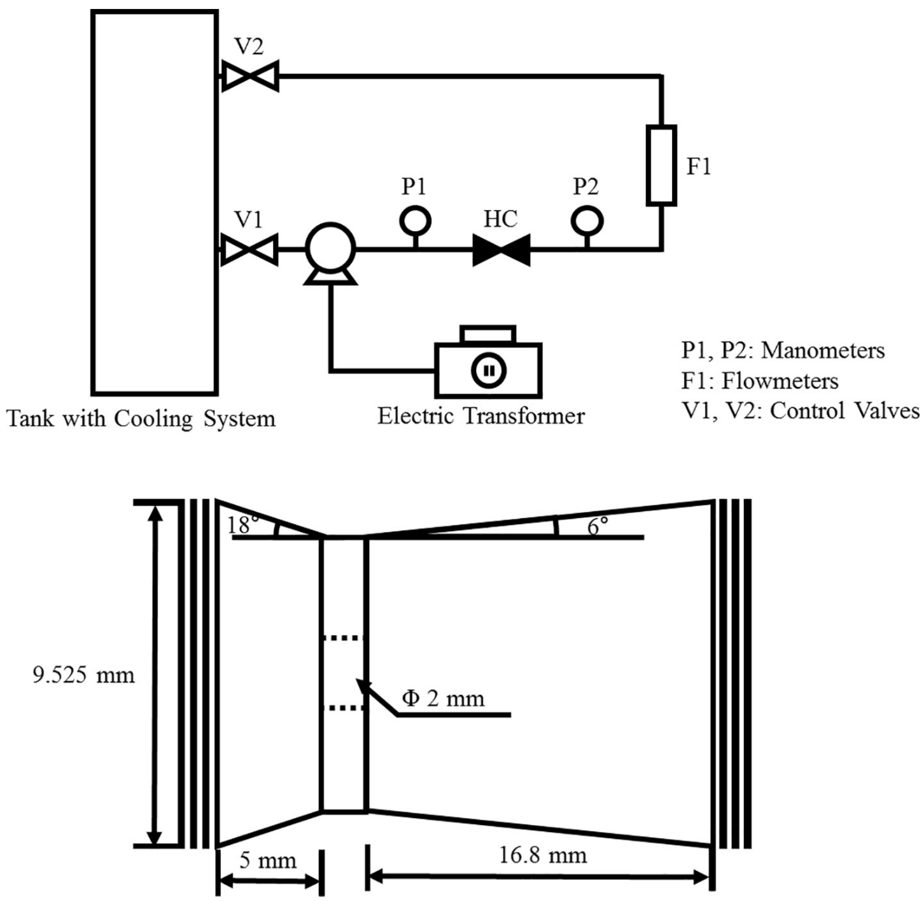

Fig. 1. Schematic diagram of an HC/PS system.

low range of approximately few ng L^{-1} – mg L^{-1} [1] although it is resistant to biodegradation. A study conducted by the US Center for Disease Control and Prevention detected BPA in 95% of urine samples from a reference population of 394 American adults at average concentrations of 1.63 mg mL^{-1} and 1.12 mg mL^{-1} in urine samples from males and females, respectively [1,2]. Additionally, several studies indicated a correlation between the exposure to BPA with sperm count reduction and increased cancer cells [3]. Therefore, there is a need for alternative processes to reduce the release and accumulation of EDCs in the environment.

BPA has a molecular weight (MW) of 228 g Mol^{-1}. It is moderately hydrophobic (water solubility 120–300 mg L^{-1}) and corresponds to a very weak acid p*Ka* 9.6–10.2 [4]. The persulfate (PS) ion ($S_2O_8^{2-}$) is a strong oxidant (E^O = 2.1 V), and it generates free $SO_4^{-}\cdot$ (E^O = 2.6 V) by breaking the O—O bond in which the bond length corresponds to 1.497 Å, [5] when activated by heat, UV, or transition metals.

Advanced oxidation processes (AOPs) are a family of technologies based on the in situ production of very reactive species, and they offer a promising alternative for wastewater treatment. Among other processes, the sulfate radical-AOP was discussed in extant studies as an efficient and affordable process. Sodium persulfate ($Na_2S_2O_8$) recently attracted the attention of the scientific community as a promising source of sulfate radicals due to its moderate cost, high stability, and aqueous solubility as well as the fact that it is a solid at ambient temperature, and this facilitates its transport and storage [6,7].

Nevertheless, PS itself is a moderate oxidizing agent and it must be activated to generate highly reactive sulfate radicals with reaction rates that are typically approximately 10^3–10^5 times faster than those of anion PS [8]. Several studies demonstrated that PS is activated by elevated temperatures (approximately 30–99 °C) [6,9,10], ultraviolet (UV)/PS process [11–14], O_3/PS process [15–16], ultrasound (US)/PS process [17–20], microwave (MW)/PS process [21], and the presence of transition metals that mainly include iron [22,23]. Specifically, Olmez-Hanci et al. [10] studied the degradation of BPA by using heat-activated or UV-activated PS. Furthermore, Darsinou et al. [18] recently showed that PS is indirectly activated by a low frequency ultrasound. The activation is potentially due to the creation of several hot spots of elevated temperature that are induced by ultrasound irradiation as well as the increase in liquid bulk temperature that is associated with heat dissipation.

In contrast to an ultrasound (acoustics), hydrodynamic cavitation (HC) generates cavitation by hydraulic pressure, generates ·OH, and also generates heat (Fig. S1).

The goal of this study involved examining the combined effects of HC and PS on the kinetics of bisphenol A degradation in relation to various operating conditions such as HC pressure, PS concentration, solution pH and temperature, and water matrix. An attempt was also made to identify transformation by-products and elucidate a plausible reaction mechanism. To the best of the authors' knowledge, this is the first report that examines the endocrine disrupting chemicals (EDCs) degradation of the HC/PS hybrid process.

2. Materials and methods

2.1. Reagent and solution preparation

Synthetic solutions for HC, PS direct oxidation, and HC based advanced oxidation were prepared by using deionized (DI) water. Bisphenol A ($C_{15}H_{16}O_2$, purity 99%, CAS number 80-05-7) and sodium persulfate ($Na_2S_2O_8$, purity 99%, CAS number 7775-27-1) with their physical–chemical properties shown in Tables S1 and S2, respectively, were purchased from Sigma Aldrich (USA). Other chemicals including NaCl (purity 99.5%), $NaHCO_3$ (purity 99.9%), $NaNO_3$ (purity 99.5%), and t-BuOH (purity 99.5%) were purchased from Sigma-Aldrich. KI (purity 99.5%) was purchased from Samchun Chemical, Korea. Additionally, 0.1 M NaOH (Duksan Pure Chemicals, Korea) was used to adjust the pH of the solution.

2.2. Experimental setup and methodology

The setup of the HC reactor is shown in Fig. 1. The reactor consists of a holding tank from where the pollutant solution is obtained, a HC reactor and an interconnecting pipeline. A reciprocating pump with a power rating of 1.1 kW is used for the recirculation of the solution through the line. The measurements of the inlet pressure and the recovered pressure were performed based on the use of pressure gauges. An orifice plate fitted in the main line has a plate thickness of 2 mm, an outer diameter of 6 mm, and a concentric hole with a diameter 2 mm that acts as a cavitating device. The HC based degradation of BPA was performed in different conditions by using a fixed solution volume of 10 L for a constant circulation time of 2 h. The temperature of the solution during the experiments approximately corresponded to 10–50 °C and was maintained by circulating cooling water through the jacket provided for the holding tank. In order to investigate the effect of pH, the initial pH was adjusted to 6, 10, and 12 by using NaOH.

2.3. Kinetic analysis and thermodynamic calculation

The kinetic constants for each test, namely the thermodynamic parameters (i.e., enthalpy, entropy, and activation energy), were determined by using the analyzed concentrations of BPA (standard curve see Fig. S2). The kinetic constants were determined by using the pseudo first order kinetic model as shown in Eq. (1) as follows:

$$\frac{dC}{dt} = -K_1 C \tag{1}$$

Here, C denotes the concentration of BPA, t denotes time, and K_1(K_{HC}, K_{PS}, *and* $K_{HC/PS}$ *system*) denotes the kinetic constant.

The half-life equation of a first order reaction is independent of the initial concentration.

$$t_{1/2} = \frac{Ln(2)}{K_1} \tag{2}$$

The synergy index is calculated by assuming that all the degradation reactions of HC, PS, and the HC/PS system follows a pseudo first order as follows:

$$\text{Synergy index (SI)} = \frac{K_{HC/PS}}{K_{HC} + K_{PS}} \tag{3}$$

where k denotes the degradation kinetic constant, and each subscript denotes each treatment process. All the experiments were repeated.

The activation parameters for the HC/PS oxidation of BPA were calculated by using the Arrhenius equation (Eq. (4)) and the Eyring equation (Eqs. (5) and (6)) [24–26] as follows:

$$\ln K = \ln A - \left(\frac{E_a}{RT}\right) \tag{4}$$

$$\ln\left(\frac{K}{T}\right) = \left(\ln\frac{K_B}{h} + \frac{\Delta S^{\#}}{R}\right) - \frac{\Delta H^{\#}}{RT} \tag{5}$$

The Gibbs free energy $\Delta G^{\#}$ is as follows:

$$\Delta G^{\#} = \Delta H^{\#} - T \times \Delta S^{\#} \tag{6}$$

where A denotes the frequency factor for the reaction, R denotes the universal gas constant (8.3144598 J mol^{-1} K^{-1}), T denotes the absolute temperature (K), K denotes the reaction rate coefficient (min^{-1}), E_a denotes the activation energy (kJ mol^{-1}), K_B denotes the Boltzmann constant (1.381×10^{-23} J K^{-1}), h denotes the Planck's constant (6.626×10^{-34} J s), $\Delta H^{\#}$ denotes the activation enthalpy (kJ mol^{-1}), and $\Delta S^{\#}$ denotes the activation entropy (J mol^{-1} K^{-1}).

2.4. Analytical methods

BPA was monitored by using high performance liquid chromatography (HPLC) (Agilent Technologies 1260 Infinity, Germany) with a C18 column (50 mm × 2.1 mm × 1.7 μm). The mobile phase, acetonitrile, and water at a ratio of 60:40 were operated in the isocratic mode with a flow rate of 0.30 mL min^{-1}, and the column and sample temperatures were fixed at 40 and 10 °C, respectively. The byproducts of BPA degradation were analyzed by using HPLC/MS (Agilent 1290 Infinity II LC/Agilent 6490 triple quadrupole LC/MS) systems in positive and negative ESI modes.

The complete mineralization was analyzed by measuring the total organic carbon (TOC) content of BPA solution using the TOC analyzer (Sievers 5310C, Laboratory TOC analyzer, USA). The NO_3^- and Cl^- anions were analyzed by using ion chromatography (ICS-1100, Dionex, USA) with an AS-19 ion-exchange column that included an AS40 automated sampler (Dionex, USA).

The KI dosimetry method was used to quantify the HC/PS reaction. The concentration of the potassium iodide (KI) (JUNSEI) solution corresponded to 10 g L^{-1}. When the KI solution irradiated with the ultrasound, iodine (I_2) was generated due to the reaction of iodide ions (I^-) and reactants (such as free radicals (•OH, •H, •OOH)) that were formed by acoustic cavitation. Iodine (I_2) reacted with the iodine ions (I^-) and generated a triiodide ion [27–28]. (I_3^-) The concentration of the triiodide ion (I_3^-) was measured by using a UV spectrophotometer (DR 6000 HACH company, USA) at a wavelength of 350 nm.

3. Results and discussion

3.1. Effect of HC inlet pressure and mechanism

Hydraulic characteristics of the cavitating device were examined by measuring the main line flow rate and by using a dimensionless parameter termed as the cavitation number (Cv). The inlet pressure to the venturi as well as flow through the main line were adjusted by changing the number of piston strokes per unit time. Cavitation number is a dimensionless number that is used to characterize the condition of cavitation in hydraulic devices [28,29]. Cavitation number is defined in Eq. (7) as follows:

$$C_v = \left(\frac{P_2 - P_v}{\frac{1}{2}\rho v_0^2}\right) \tag{7}$$

where Cv denotes the Cavitation number*;* P_2 denotes fully recovered downstream pressure (Pa)*;* p_v denotes vapor pressure of the fluid (Pa)*;* ρ denotes density of the fluid (kg m^{-3})*;* and v_0 = velocity of the fluid (m s^{-1}). Under ideal conditions, cavities are generated at a condition corresponding to $C_v < 1$. However, in several cases, cavities are generated at a value of C_v that exceeds one due to the presence of some dissolved gases and suspended particles that provide additional nuclei for the cavities as noted by Saharan et al. [30] and Shah et al. [31].

Hence, Cv decreased from 1.12 to 0.68 when the pressure increased from 0.3 MPa to 0.7 MPa as shown in Table 1 and Fig. 2 (A) while •OH generation corresponded to 0.129 (R^2: 0.91) μM min^{-1}, 0.219 (R^2: 0.97) μM min^{-1}, and 0.147 (R^2: 0.92) μM min^{-1}, and the highest •OH generation value was observed when the inlet pressure corresponded to 0.5 MPa.

Additionally, the results of applying HC, PS, and HC/PS processes at the optimum pressure of 0.5 MPa as derived from Fig. 2(B) show that the oxidation kinetic constants of BPA are 1.0×10^{-3} min^{-1}, 4.7×10^{-3} min^{-1}, and 12.7×10^{-3} min^{-1} (Eq. (1)), respectively, and the half-life ($t_{1/2}$) correspond to 693 min, 147 min, and 55 min (Eq. (2)) respectively. Furthermore, the synergy index (SI) is 2.23 (Eq. (3)).

An increase in the venturi inlet pressure decreases the cavitation number, and this increases the number of cavities that are formed. However, at the operating condition of the inlet pressure exceeding

Table 1
Flow characteristics of the cavitation reactor (Orifice diameter of 2 mm).

Inlet pressure (MPa)	Volume (L)	Temperature (°C)	pH	Reaction time (min)	Flow rate ($L\,min^{-1}$)	Velocity ($m\,s^{-1}$)	Cavitation number (C_V)	Power dissipated P_D (W)	·OH production ($\mu M\,min^{-1}$)
0.3	10	50 ± 0.5	6 ± 0.5	120	3.79	8.86	1.12	124	0.129
0.5					4.16	9.72	1.02	192	0.223
0.7					5.68	13.28	0.68	295	0.147

0.5 MPa, the density of cavities is extremely high such that the entire downstream area is filled with cavities, and the cavities then begin to coalesce with each other and form a cavity cloud [30].

In Eqs. (8)(12), when cavitation occurs owing to the pressure difference of HC, it releases ·OH as well as a large amount of energy (Eq. (8)). The emitted energy converts $S_2O_8^{2-}$ to $SO_4^-\cdot$ (Eq. (9)), and $SO_4^-\cdot$reacts with water to generate ·OH with stronger oxidation (Eq. (10)). Specifically, it transforms to ·OH under alkaline conditions (Eq. (11)). The generated ·OH reacts with SO_4^{2-} (Eq. (12)). The reaction rate difference corresponds to the reaction rate constant of $SO_4^-\cdot$ and OH^-, and it is 100 times faster than the rate constant of the reaction between ·OH and SO_4^{2-}. Therefore, it is considered that the processes that combine HC and PS exhibit synergy. The expressions are as follows:

$$H_2O \xrightarrow{HC} \cdot OH + \cdot H + heat \tag{8}$$

$$S_2O_8^{2-} + \text{heat} \rightarrow 2\,SO_4^{-}\cdot \tag{9}$$

$$SO_4^{-}\cdot + H_2O \rightarrow \cdot OH + SO_4^{2-}\ (k < 60 M^{-1} S^{-1}) \tag{10}$$

$$SO_4^{-}\cdot + OH^- \rightarrow \cdot OH + SO_4^{2-}\ (k = 6.5 \times 10^7 M^{-1} S^{-1}) \tag{11}$$

$$\cdot OH + SO_4^{2-} \rightarrow SO_4^{-}\cdot + OH^-\ (k = 3.5 \times 10^7 M^{-1} S^{-1}) \tag{12}$$

Specifically, t-BuOH that acts as a scavenging agent for ·OH was used to investigate the oxidation mechanism of BPA in the HC/PS system. The second order rate constant of t-BuOH that reacts with $SO_4^-\cdot$ ($K_{SO4\text{-}\cdot,\ t\text{-}BuOH} = 8.4 \times 10^5 M^{-1} s^{-1}$ at pH 7) [32] is almost three orders of magnitude lower than that with ·OH ($K_{OH\cdot,\ t\text{-}BuOH} = 6.0 \times 10^8 M^{-1} s^{-1}$ at pH 7) [32]. Thus, t-Butanol was selected as the ·OH quenching reagent to determine the second order rate constant between BPA with $SO_4^-\cdot$ when BPA was used as a reference compound.

$$K_{obs,HC/PS} = K_{obs,HC} + K_{SO_4^-\cdot} C_{SO_4^-\cdot,HC/PS} + K_{\cdot OH} C_{\cdot OH,HC/PS} \tag{13}$$

Given the scavenging of ·OH by t-BuOH, Eq. (13) is simplified to Eq.

Table 2
Observed HC based pseudo first order rate constant at the reaction conditions (BPA = 0.044 mM, PS = 0.70 mM, t-BuOH = 4.38 mM, P = 0.5 MPa, pH = 6, and T = 50 °C).

Pollutants	K_{obs}($\times 10^{-3} min^{-1}$)		Contribution to HC/PS (%)	
	HC only	HC/PS	·OH	$SO_4^-\cdot$
BPA	1.0	12.7	10.32	89.68
	HC/t-BuOH	HC/PS/t-BuOH		
	0	11.3		

(14) as follows:

$$K_{obs,HC/PS} = K_{obs,HC} + K_{SO_4^-\cdot} C_{SO_4^-\cdot,HC/PS} \tag{14}$$

The results are presented in Fig. 2(B) and Table 2. In the case with only HC and HC/t-BuOH, the oxidation rate constants of BPA corresponded to 1×10^{-3} and $0\ min^{-1}$, respectively. Additionally, with HC/PS and HC/PS/t-BuOH, the oxidation rate constants of BPA corresponded to 12.7×10^{-3} and 11.3×10^{-3}, respectively. Therefore, $SO_4^-\cdot$ is considered as the main oxidation mechanism of BPA in the HC/PS processes when t-BuOH (an ·OH scavenging agent) is injected. The contribution of ·OH, and $SO_4^-\cdot$ oxidation to BPA oxidation corresponded to 10.3% and 89.7%, respectively.

3.2. Effect of PS concentration

$S_2O_8^{2-}$ is a strong oxidant, and thus it generates free $SO_4^-\cdot$ by breaking the O—O bond, [5] when activated by heat, UV, or transition metals. When the concentration of pollutants is constant, the reaction rate of pollutants is influenced by the concentration of oxidized PS. In the study, we investigated the oxidation ability of BPA based on the injected concentration of PS given the HC injection pressure of 0.5 MPa, temperature of 50 °C, and a pH of 6 as shown in Fig. 4.

As shown in Fig. 3(A), when the PS concentrations corresponded to 0 mM, 0.31 mM, 0.61 mM, 0.70 mM, 1.39 mM, 2.78 mM, and 4.17 mM,

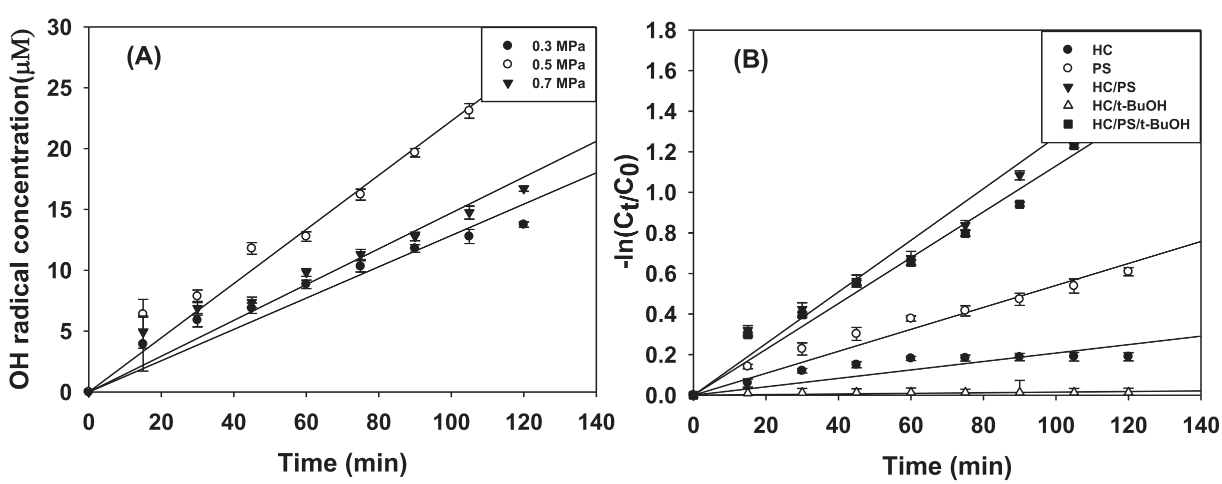

Fig. 2. (A) ·OH generation owing to the inlet pressure in the HC system (B) BPA reaction rate based on the HC, PS, and HC/PS system (Temperature = 50 °C, Pressure = 0.5 MPa, BPA = 0.044 mM, PS = 0.700 mM, t-BuOH = 4.380 mM, and pH = 6).

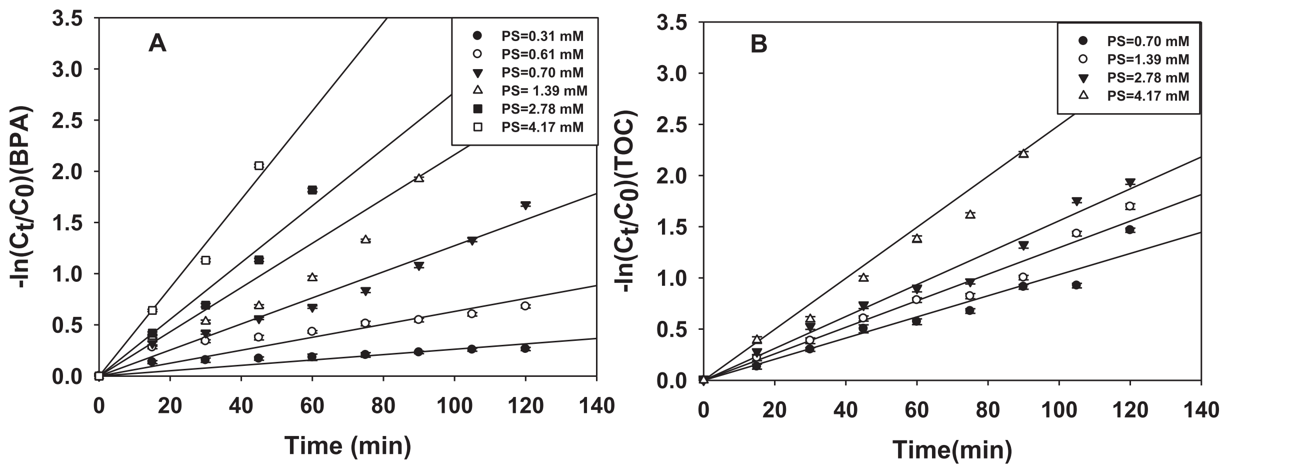

Fig. 3. Pseudo first order kinetics plots of BPA degradation data with different initial PS concentrations at BPA = 0.044 mM, HC pressure = 0.5 MPa, Temperature = 50 °C, and pH = 6.

the reaction rate constant values corresponded to 1.0, 1.8, 4.7, 12.3, 22.3, 29.0 and 43.2 × 10^{-3} min^{-1}, respectively. The half-life ($t_{1/2}$) time values corresponded to 693 min, 385 min, 147 min, 55 min, 31 min, 23.9 min, and 16 min, respectively. Additionally, the correlation between the PS concentration and the BPA reaction rate constant in Fig. 3(A) was calculated as K_{BPA} = 10.854 × PS concentration (R^2: 0.941).

Fig. 3(B) shows that the BPA (TOC) reaction rate constants correspond to 10.3, 13.0, 15.6 and 24.9 × 10^{-3} min^{-1}, when the PS concentrations correspond to 0.70 mM, 1.39 mM, 2.78 mM, and 4.17 mM, respectively. The half-life ($t_{1/2}$) time values correspond to 67 min, 53 min, 44 min, and 28 min. Olmez-Hanci et al. [10] studied BPA oxidation based on the PS concentration (5, 10, 20 mM) at BPA 20 mg L^{-1}, pH 6.5, and a temperature of 60 °C. However, at concentrations that exceed a specific concentration, the PS concentration exhibit scavenging in the $SO_4^{-}\cdot$ formation as shown in Eqs. (15) and (16). In the study, the PS concentration was below 5 mM, and the rate constant of BPA increased with increases in the initial PS concentration. The expressions are as follows:

$$SO_4^{-}\cdot + S_2O_8^{2-} \rightarrow SO_4^{2-} + S_2O_8^{-}\cdot (k = 6.1 \times 10^5\ M^{-1}\ S^{-1}) \quad (15)$$

$$SO_4^{-}\cdot + SO_4^{-}\cdot \rightarrow S_2O_8^{-}\ (k = 4.0 \times 10^8\ M^{-1}\ S^{-1}) \quad (16)$$

3.3. Effect of pH

The solution pH is an important factor in determining the physical and chemical properties of the solution that influence the oxidation kinetic constant. The effect of pH on oxidation rate was examined at pH 6, pH 10, and pH 12.

The results are illustrated in Fig. 4, the gage inlet pressure was fixed at the optimized value of P_{in} = 0.5 MPa, and the temperature corresponded to 50 °C. The kinetic constants of BPA at pH 6, pH 10, and pH 12 were 12.3 × 10^{-3} (R^2: 0.97), 5.8 × 10^{-3} (R^2: 0.92) and 3.2 × 10^{-3} (R^2:0.82), respectively, and the rate constant was decreased with increases in the pH.

The examined BPA molecule corresponded to a non-volatile compound and the region of degradation was outside the cavitation bubble. The BPA concentration at the hydrophobic bubble interface is clearly influenced by the solution pH above its p*Ka* value. A potential explanation may involve the ionization state of BPA in which the p*Ka* value is approximately in the range of 9.9–11.3 [33]. The detrimental effect of alkaline conditions was more pronounced for the experiment in the presence of PS since a pH increase from 6 to 12 led to a decrease by 4.1 times. This is potentially because the PS is less negatively charged at acidic conditions as opposed to alkaline conditions. Consequently, it

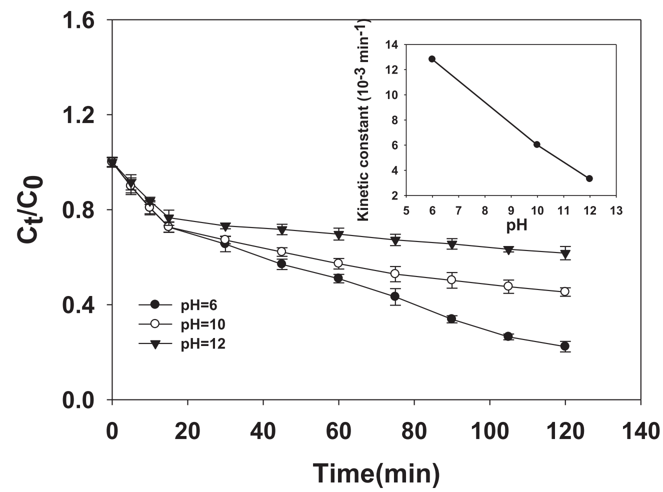

Fig. 4. Effect of initial pH on 0.044 mM BPA, HC/PS at 0.5 MPa pressure, and temperature control at 50 °C with 0.70 mM PS.

can diffuse faster towards the negatively charged cavitation bubble.

The oxidation rates in both HC/PS processes decreased from pH 6 to pH 12, and this is possibly due to the decrease in the redox potential of $\cdot OH/H_2O$ with the increase in pH. For example, based on Eqs. (17)(19) (derived from the Nernst equation), the redox potential of $\cdot OH/H_2O$ at pH 6, pH 10, and pH 12, are 2.446 V, 2.21 V, and 2.092 V, respectively, and of $SO_4^{-}\cdot/H_2O$ correspond to 2.246 V, 2.01 V, and 1.892 V, respectively. The expressions are as follows [34,35]:

$$E^0_{\cdot OH/H_2O} = 2.8\ V \quad (17)$$

$$E^0_{SO_4^{-}\cdot/H_2O} = 2.6\ V \quad (18)$$

$$E_{\cdot OH(SO_4^{-}\cdot)} = E^0_{\cdot OH(SO_4^{-}\cdot)/H_2O} - 0.059pH \quad (19)$$

In the HC/PS process, the degradation rates increased slightly under the acidic condition. This is because a lower amount of $SO_4^{-}\cdot$ is transformed to $\cdot OH$ at a lower pH (Eqs. (20) and (21)). Thus, $SO_4^{-}\cdot$ is the predominant radical species in the HC/PS process under the acidic condition. In contrast, a high alkaline condition by a pH above 10, the major radical species in the HC/PS process is $\cdot OH$ (Eqs. (11) and (12)). Thus, the degradation rates also decreased with increases in the pH in the HC/PS process because $SO_4^{-}\cdot$ is more reactive when compared to $\cdot OH$ with BPA. The expressions are as follows [36,37]:

$$SO_4^{-}\cdot + H_2O \rightarrow \cdot OH + SO_4^{2-} + H^+ \quad (k = 60\ M^{-1}\ S^{-1}) \quad (20)$$

$$SO_4^{-}\cdot + H_2O \rightarrow \cdot OH + HSO_4^{-} \quad (k = 500\ S^{-1}) \quad (21)$$

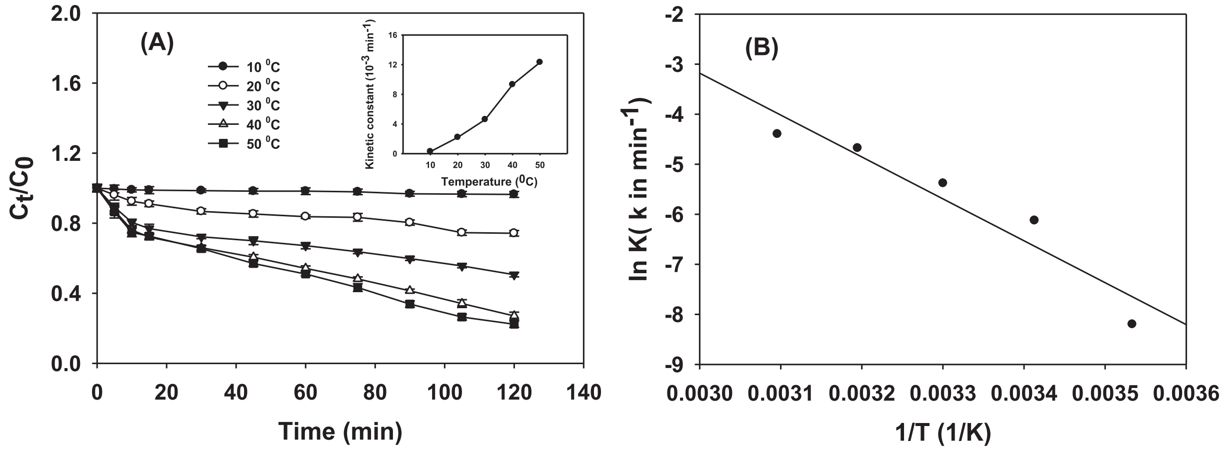

Fig. 5. Pseudo fist order kinetic plots (A) of BPA degradation by HC/PS with different temperature (10–50 °C) at pH = 6, HC = 0.5 MPa, BPA = 0.044 mM, and PS = 0.70 mM. An Arrhenius plot of the pseudo first order kinetic constants (B) yields the apparent activation energy for the degradation of BPA by HC/PS.

3.4. Effect of temperature

Temperature is an important parameter in the oxidation process because it affects the activation energy as well as pollutant behavior. As a result, the rate constants at 10 °C, 20 °C, 30 °C, 40 °C, and 50 °C were 0.28×10^{-3} (R^2: 0.95), 2.2×10^{-3} (R^2: 0.94), 4.6×10^{-3} (R^2: 0.93), 9.3×10^{-3} (R^2: 0.97), and 12.3×10^{-3} (R^2: 0.97) min^{-1}, respectively. Accordingly, the rate constants increased when the temperature increased as shown in Fig. 5(A). The Arrhenius equation is used, and the calculated activation energy (*Ea*) corresponded to 69.62 kJ mol^{-1} (Fig. 5(B)). This is less than the values of Ea 184 ± 12 kJ mol^{-1} and 119 ± 10.8 kJ mol^{-1} in the BPA oxidation by using PS as proposed by Olmez-Hanci et al. [10] and Gauch and Tuqan [38]. In chemistry, the activation energy is the minimum energy that must be available to a chemical system with potential reactants to result in a chemical reaction [39]. Therefore, a decrease in the Ea value decreases the energy required for BPA oxidation and decreases the costs of the process, thereby making it more economical. Additionally, based on the Eyring equation (Eqs. (2)(4)), the calculated $\Delta H^{\#}$ and $\Delta S^{\#}$ correspond to 72.13 kJ mol^{-1} and 0.041 kJ mol^{-1} K^{-1}, respectively, and the relationship between $\Delta G^{\#}$ and temperature is shown in Eq. (22). Therefore, an increase in temperature increased $\Delta G^{\#}$ and the reaction rate. The expressions are as follows:

$$\Delta G^{\#} = 72.13\text{–}0.041 \times T\,(kJ\ mol^{-1}) \tag{22}$$

3.5. Effect of aqueous matrix species

A few matrix species that are commonly present in water react with radical species including $SO_4^{-}\cdot$ and $\cdot OH$ in competition with the target pollutants [40,41]. Therefore, it is very important to examine the manner in which any negative ions in water affect the reaction.

In the study, the effect of single anions and mixed anions on the rate of BPA oxidation in the HC/PC process was investigated as shown in Fig. 6.

As a result, the BPA oxidation rate constant was obtained when the concentration of Cl^- (pH = 3.16), NO_3^- (pH = 3.64), and HCO_3^- (pH 6 ± 0.5) corresponded to 0.32 mM at the inlet pressure of 0.5 MPa with 0.70 mM PS and pH 6. The negative ion order that positively affects the kinetic constant corresponds to 27×10^{-3} (R^2: 0.855), 19.5×10^{-3} (R^2: 0.878), and 12.3×10^{-3} min^{-1}, in which $Cl^- > NO_3^- > HCO_3^-$.

The redox potential values of the radicals participating in the reaction are as follows: $E^0\cdot_{OH} = 2.8$ V, $E^0_{SO4-}\cdot = 2.6$ V [8], $E^0_{1/2CO3-}\cdot = 1.5$ V; $E^0_{1/2Cl2-}\cdot = 2.09$ V; and $E^0_{1/2NO3}\cdot = 2.5$ V [42,43].

In the reaction of $\cdot OH$ and chlorine ions in Eqs. (23) and (24), the chlorine ion produces more $\cdot OH$ (about 28%) by catalysis, and thus the

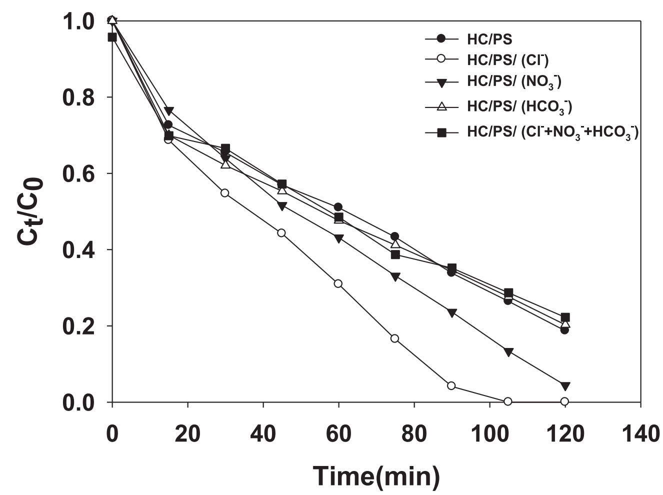

Fig. 6. Effect of anions on BPA oxidation by using HC/PS processes. Experimental conditions: (BPA = 0.044 mM, Cl^-, NO_3^-, and HCO_3^- = 0.32 mM, HC = 0.5 MPa, PS = 0.70 mM, pH = 6, and Temp. = 50 °C).

reaction rate constant (27.0×10^{-3} min^{-1}) is approximately 52.96% faster than the reaction rate constant (12.7×10^{-3} min^{-1}) for BPA oxidation by using HC/PS processes. The expressions are as follows [32,44]:

$$\cdot OH + Cl^- \rightarrow ClOH^-\cdot \quad (k = 4.3 \times 10^9\ M^{-1}\ S^{-1}) \tag{23}$$

$$ClOH^-\cdot \rightarrow \cdot OH + Cl^- \quad (k = 6.0 \times 10^9\ M^{-1}\ S^{-1}) \tag{24}$$

In Eqs. (25) and (26), the rate constants of $SO_4^{-}\cdot$ and Cl^- and the rate constants of $\cdot Cl$ and Cl^- were similar. Additionally, it was demonstrated that $Cl_2^{-}\cdot$ presents rate constants when they react with the oxygenated hydrocarbons ranging from $1.4 \times 10^3\ M^{-1}\ s^{-1}$ to $2.7 \times 10^5\ M^{-1}\ s^{-1}$ [45] and with amino acids ranging from $1.2 \times 10^5\ M^{-1}\ s^{-1}$ to $1.4 \times 10^7\ M^{-1}\ s^{-1}$ [42]. This indicates that $Cl_2^{-}\cdot$ can sometimes selectively react with an organic compound at comparable rates in a manner similar to $SO_4^{-}\cdot$ (as in the case of serine amino acid with $2.3 \times 10^7\ M^{-1}\ s^{-1}$) [42]. The expressions are as follows [46,47]:

$$SO_4^{-}\cdot + Cl^- \rightarrow Cl\cdot + SO_4^{2-} \quad (k = 3.1 \times 10^8\ M^{-1}\ S^{-1}) \tag{25}$$

$$Cl\cdot + Cl^- \leftrightarrow Cl_2^{-}\cdot \quad (k = 5.7 \times 10^9, 7.8 \times 10^9\ M^{-1}\ S^{-1}) \tag{26}$$

The kinetic constants of BPA oxidation by using $HC/PS/NO_3^-$ and HC/PS processes were 19.5×10^{-3} and 12.7×10^{-3} min^{-1}, respectively, and the reaction rate of $HC/PS/NO_3^-$ process was approximately 38.7% higher than that of the HC/PS process.

According to Exner et al. [43], $NO_3\cdot$ exhibited the highest K_{obs} at approximately $5.0 \pm 0.5 \times 10^4\,M^{-1}\,s^{-1}$ in a solution containing NO_3^- as shown in Eqs. (27) and (28).

Furthermore, the $NO_3\cdot$ redox potential ($E^0_{1/2NO3} = 2.5\,V$) was high, and Eqs. (17)(19) were used to calculate the $\cdot OH$ and $SO_4^-\cdot$ redox potentials at the initial pH values corresponding to 3.64 and 6.0 as 2.585 ($\cdot OH$) and 2.385 ($SO_4^-\cdot$) V and 2.446($\cdot OH$) and 2.246 ($SO_4^-\cdot$) V, respectively, for the HC/PS/NO_3^- and HC/PS. It is considered that the $\cdot OH$ and $SO_4^-\cdot$ redox potential values in the HC/PS/NO_3^- process exceed those in the HC/PS process. The expressions are as follows [43]:

$$\cdot OH + NO_3^- \rightarrow NO_3\cdot + OH^- \quad (27)$$

$$SO_4^-\cdot + NO_3^- \rightarrow NO_3\cdot + SO_4^{2-} \quad (k = 5.0 \times 10^4\ M^{-1}\ S^{-1}) \quad (28)$$

The HCO_3^- is known for its capacity to quench sulfate radicals and hydroxyl radicals as well with rate constants of approximately $8.5 \times 10^6\,M^{-1}\,s^{-1}$ (Eq. (29)) and $9.1 \times 10^6\,M^{-1}\,s^{-1}$ (Eq. (30)), respectively. However, in the study, the reaction rate constant in the presence of HCO_3^- ion was $12.3 \times 10^{-3}\,min^{-1}$, and this is similar to that of DI water at $12.7 \times 10^{-3}\,min^{-1}$. Nevertheless, the cause was not identified. The expressions are as follows [32]:

$$\cdot OH + HCO_3^- \rightarrow CO_3^-\cdot + H_2O \quad (k = 8.5 \times 10^6\ M^{-1}\ S^{-1}) \quad (29)$$

$$SO_4^-\cdot + HCO_3^- \rightarrow CO_3^-\cdot + HSO_4^- \quad (k = 9.1 \times 10^6\ M^{-1}\ S^{-1}) \quad (30)$$

Fig. 7 also shows the effect of HC/PS process on the oxidation of BPA when Cl^-, NO_3^-, and HCO_3^- (0.32 mM, pH = 6 ± 0.2) were mixed. As a result, 3.2% of reduction was founded by comparing with the oxidation rate constant for all types of anions ($12.7 \times 10^{-3}\,min^{-1}$, R^2: 0.970) and that of the anion-free BPA ($12.3 \times 10^{-3}\,min^{-1}$, R^2: 0.980). The reason for this is unclear, but it can be thought that the positive reaction and the negative reaction occurs at the same time because of the reasons that mentioned previous paragraphs.

3.6. Study of transformation and by-products

The HC/PS degradation of BPA was investigated in the HC reactor at 0.5 MPa HC inlet pressure and 0.70 mM PS concentration as shown in Fig. 7.

The degradation of BPA was quantified after 30 min, 60 min, 90 min, and 120 min of the HC/PS system, and the degradation efficiencies based on BPA concentrations removal were obtained at 34.51%, 49.02%, 66.16%, and 81.28% respectively. The mineralization of BPA was quantified after 30 min, 60 min, 90 min, and 120 min of the HC/PS system, and the mineralization efficiencies based on TOC concentration removal were obtained at 26.00%, 43.57%, 59.86%, and 76.92%, respectively (Fig. 7(A)).

The TOC was not completely removed and it was not possible to preclude the generation of compounds that are more hazardous when compared to the initial contaminant, BPA, thus the main BPA by-products formed during the HC/PS degradation were identified. The study was performed by using HPLC/MS in both positive and negative electrospray modes. The TOC samples that are obtained after 30 min, 60 min, 90 min, and 120 min of the HC/PS system, were used in the analysis of byproducts (Fig. 7(B)). Fig. 7(B) shows the extracted ion chromatography peak areas of these productions based on the irradiation time. In the study, the five main intermediates produced by HC/PS system corresponded to monohydroxylated bisphenol A ($C_{15}H_{16}O_3$), 4-isopropenylphenol ($C_9H_{10}O$), 4-hydeoxyacetophenone $C_8H_8O_2$), quinone of monohydroxylated bisphenol A ($C_{15}H_{14}O_3$), and dihydroxylated bisphenol A ($C_{15}H_{16}O_4$) (Table S3). The main intermediates $C_8H_8O_2$ increased to 40 min and then decreased while the intermediate $C_9H_{10}O$ continuously increased to 120 min. The intermediate $C_{15}H_{14}O_3$ also increased to 40 min and then decreased. The remaining $C_{15}H_{16}O_3$ and $C_{15}H_{16}O_4$ increased to 30 min and was then maintained for 120 min.

Therefore, further degradation of the ring rupturing process produced $C_8H_8O_2$, $C_9H_{10}O$, and $C_8H_6O_2$ intermediates that corresponded to aliphatic compounds that were comprised of carboxylic acid (including hexanoic acid, succinic acid, and fumaric acid oxalic acid) [48]. Subsequently, the produced carboxylic acid is further degraded, and this is followed by the evolution of CO_2 and H_2O.

Generally, $SO_4^-\cdot$ is more likely to participate in electron transfer reactions as opposed to OH, which is more likely to participate in hydrogen abstraction or addition reactions [49]. Specifically, $SO_4^-\cdot$ is selective radical which prefer to react with the aromatic ring while $\cdot OH$ is non-selective one which reacts with both the aromatic ring and the aliphatic chain. Although $\cdot OH$ are non-selective, some discrimination exists in practice among potential sites of attack [48]. The existence of electron-donating OH group increases the electron density of the aromatic ring and renders the double bond more vulnerable to the electrophile attack [49]. Thus, it is assumed that the degradation of BPA proceeds mainly through the attack of the electrophilic $\cdot OH$ on the phenyl groups of BPA. Attack of the $\cdot OH$ on the aromatic ring of BPA is expected to occur preferentially at the ortho position due to the *ortho*-orientation and *para*-orientation tendency of the ring OH group. The production of radicals ($SO_4^-\cdot$ and $\cdot OH$) and the formation of (hydroxyl) BPA radical during sono and UV-activated PS with BPA was emphasized in a recent study [18,50]. Heated PS [10,38], and

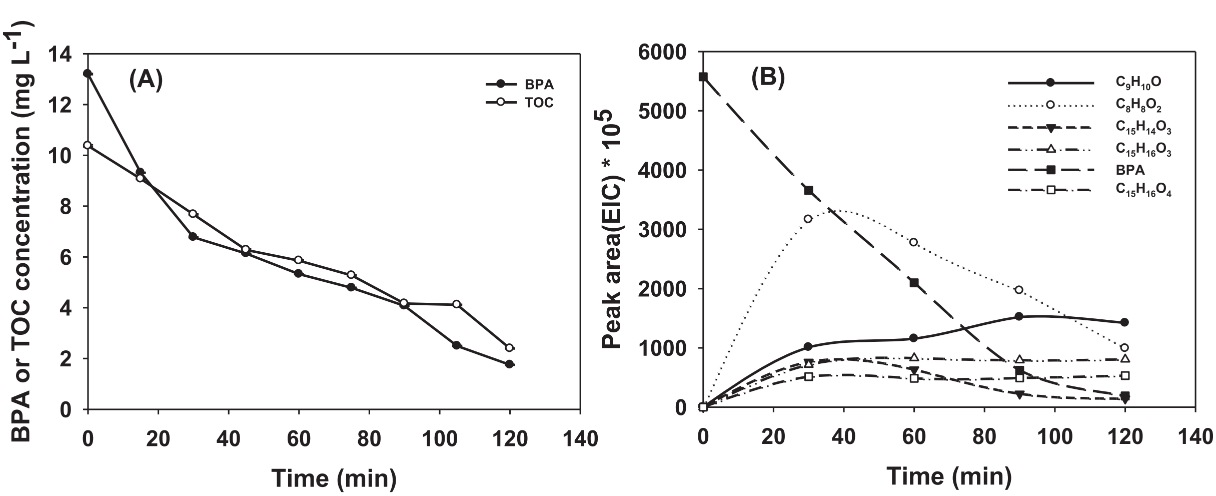

Fig. 7. (A) Profiles of BPA and TOC removal during the HC/PS system (B) Intermediate formation of BPA oxidation at HC/PS applications under optimum condition: (BPA = 0.044 mM, HC/PS processes = 0.5 MPa, temperature = 50 °C, pH = 6, and PS = 0.70 mM).

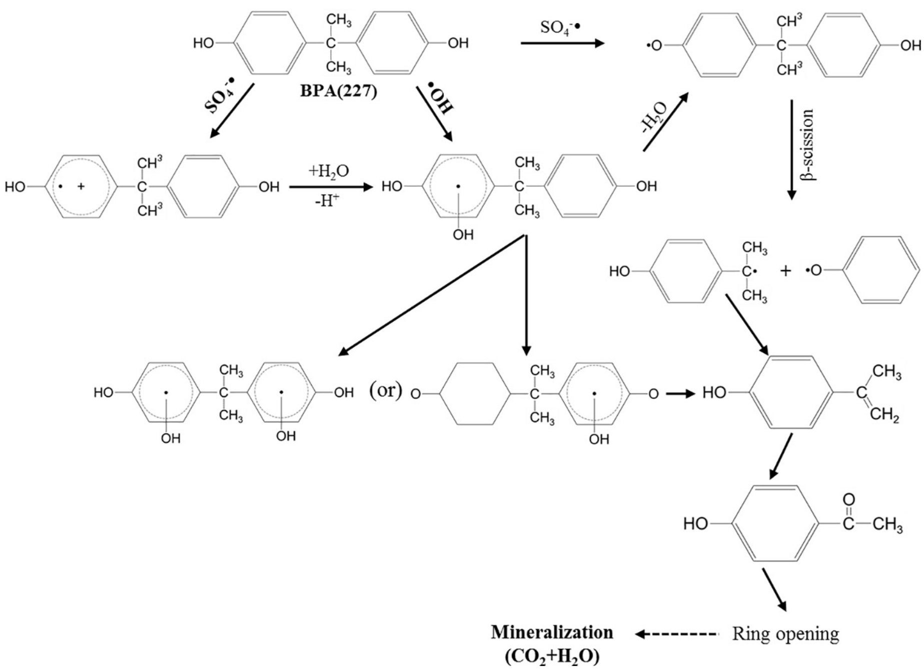

Fig. 8. Cleavage pathways of BPA HC/PS degradation (BPA = 0.044 mM, HC/PS processes = 0.5 MPa, temperature = 50 °C, pH = 6, and PS = 0.70 mM).

Table 3
Economic comparison of HC, PS, and HC/PS processes for BPA removal in DI water.

	PS Conc. (mmol L^{-1})	Kinetic constant (10^{-3} min^{-1})	EEO (KWh m^{-3} $order^{-1}$)	Cost (\$ m^{-3} $order^{-1}$)			Condition
				HC[a]	PS[b]	Total	
HC	–	2.6	284	37.4	–	37.4	BPA = 10 mg L^{-1}
PS	0.7	4.7	–		35.4	35.4	Pressure = 0.5 MPa
HC/PS	0.31	1.8	410	54.0	41.0	95.0	Power = 192 W
	0.61	4.7	157	20.7	30.9	51.6	Temperature = 50 °C
	0.70	12.6	58.5	7.72	13.2	20.9	pH = 6
	1.39	22.3	33.1	4.36	14.8	19.2	
	2.78	29	25.4	3.35	22.8	26.2	
	4.17	43.2	17.1	2.25	23.0	25.2	

[a] Electrical energy cost = 0.1319 \$ $(kWh)^{-1}$ [57].
[b] $Na_2S_2O_8$ (99%) cost = 1.00 \$ kg^{-1} [58].

sonochemical oxidation [51,52] also clearly show the importance of radicals and by-products during the treatment. The data suggests that BPA is potentially concentrated on the HC/PS treatment where it is readily degraded by $\cdot OH$, and $SO_4^-\cdot$ plays an important role in initiating sequential ring cleavage via hydroxylation on the aromatic rings. The detection of partially hydroxylated aromatic compounds and ring ruptured products were reported in several studies [53,54].

The pathway is rationalized through the elimination of water from the (hydroxyl) BPA radical to form the (phenoxyl) BPA radical that is followed by b-scission to finally produce isopropenylphenol and phenoxy radicals (Fig. 8) as also reported by other extant studies [49]. The analysis result produces $C_8H_8O_2$, $C_9H_{10}O$, and $C_{15}H_{14}O_3$ intermediates. The advantage of using an HC/PS system corresponds to the synergistic index of each process that allows complete degradation of BPA as well as both hydrophilic and hydrophobic intermediates without producing toxic byproducts.

3.7. Economic comparison of HC/PS processes

An economic comparison of HC/PS processes for removal of BPA was conducted based on the total cost of electrical energy and the oxidants. The electrical energy per order (EEO) (kWh m^{-3}) is calculated from Eqs. (31) and (32) as follows:

$$EEO = \frac{P \times t \times 1000}{V \times 60 \times \log\left(\frac{C_i}{C_f}\right)} \tag{31}$$

$$\text{In}\left(\frac{C_i}{C_f}\right) = K \times t \tag{32}$$

where P denotes the HC power input (kW) of the HC/PS system, t denotes the irradiation time (h), V denotes the treated water volume (L), K denotes the first order rate constant (min^{-1}), and C_i and C_f denote the initial and final pollutant concentrations (mg L^{-1}), respectively [55–56]. From Eqs. (31) and (32), EEO is expressed as follows (Eq. (33)):

$$EEO = \frac{38.4 \times P}{V \times K} \tag{33}$$

The results indicate that Eq. (32) in the HC, PS, and HC/PS processes during BPA degradation. EEO and total cost are presented in Table 3. However, in the HC/PS processes, the BPA kinetic constant was increased with increases in the PS concentration while the EEO and total cost values decreased.

4. Conclusions

This study involved investigating the effect of varying operating parameters, including temperature, pH, and oxidant concentration, on the HC/PS process treatment of a potentially endocrine disrupting BPA compound. Following the optimization of the treatment performance, BPA degradation products that were formed during HC/PS process degradation were quantified via LC–MS to examine the relationship between HC/PS oxidation products. The main conclusions are as follows:

(1) HC by itself degrades BPA at the conditions employed in the study. However, the synergy index effect of HC/PS degradation that results in the formation of hydroxyl and sulfate radicals is beneficial for the oxidation of BPA.
(2) During the BPA degradation by using the HC/PS process, the mechanism corresponded to $\cdot OH$ and $SO_4^-\cdot$ degrading although the main degradation mechanism corresponded to $SO_4^-\cdot$.
(3) The kinetic constant of BPA oxidation decreased with increases in the pH and increased with increases in the temperature.
(4) The environmental matrix containing other anionic radical scavengers affects the decomposition kinetics when compared to operations in deionized water. Chloride ion also acts as a catalyst to increase the amount of $\cdot OH$ and to increase the oxidation kinetic constant.
(5) Intermediates of BPA degradation were identified and BPA degradation pathways were proposed based on the HPLC-MS analytical data.
(6) HC/PS system was more cost effective with respect to the reaction conditions adopted in the study.

HC/PS system has benefits in future applications. Because it is an AOP process that can be applied with very little operating cost and simple equipment.

Acknowledgement

This study was supported by the National Research Foundation (NRF-2017R1D1A1B03030079) and Korea Institute of Energy Technology Evaluation and Planning (KETEP, 20152510101820).

Appendix A. Supplementary data

Supplementary data associated with this article can be found, in the online version, at http://dx.doi.org/10.1016/j.cej.2018.01.018.

References

[1] L.N. Vandenberg, R. Hauser, M. Marcus, N. Olea, W.V. Welshons, Human exposure to bisphenol A (BPA), Reprod. Toxicol. 24 (2007) 139–177.
[2] A.M. Calafat, Z. Kuklenyik, J.A. Reidy, S.P. Caudill, J. Ekong, L.L. Needham, Urinary concentrations of bisphenol A and 4-nonylphenol in a human reference population, Environ. Health Perspect. 113 (2005) 391–395.
[3] S. Salian, T. Doshi, G. Vanage, Perinatal exposure of rats to bisphenol A affects the fertility of male offspring, Life Sci. 85 (2009) 742–752.
[4] C.A. Staples, P.B. Dorn, G.M. Klecka, S.T. O'Block, L.R. Harris, A review of the environmental fate, effects, and exposures of bisphenol A, Chemosphere 36 (1998) 2149–2173.
[5] M.G. Antoniou, A.A. de la Cruz, D.D. Dionysiou, Degradation of microcystin-LR using sulfate radicals generated through photolysis, thermolysis and e^- transfer mechanisms, Appl. Catal., B 96 (2010) 290–298.
[6] Z. Frontistis, E.M. Mestres, I. Konstantinou, D. Mantzavinos, Removal of cibacron black commercial dye with heat- or iron-activated persulfate: statistical evaluation of key operating parameters on decolorization and degradation by-products, Desalin. Water Treat. 57 (2016) 2616–2625.
[7] Y.T. Lin, C. Liang, J.H. Chen, Feasibility study of ultraviolet activated persulfate oxidation of phenol, Chemosphere 82 (2011) 1168–1172.
[8] A. Tsitonaki, B. Petri, M. Crimi, H. Mosbaek, R.L. Siegrist, P.L. Bjerg, In situ chemical oxidation of contaminated soil and groundwater using persulfate: a review, Crit. Rev. Environ. Sci. Technol. 40 (2010) 55–91.
[9] Y. Ji, C. Dong, D. Kong, J. Lu, Q. Zhou, Heat-activated persulfate oxidation of atrazine: Implications for remediation of groundwater contaminated by herbicides, Chem. Eng. J. 263 (2015) 45–54.
[10] T. Olmez-Hanci, I. Arslan-Alaton, B. Bora, Genc, Bisphenol A treatment by the hot persulfate process: oxidation products and acute toxicity, J. Hazard. Mater. 263 (2013) 283–290.
[11] Y. Xiao, L. Zhang, W. Zhang, K.Y. Lim, R.D. Webster, T.T. Lim, Comparative evaluation of iodoacids removal by UV/persulfate and UV/H_2O_2 processes, Water Res. 102 (2016) 629–639.
[12] Y. Qian, X. Guo, Y. Zhang, Y. Peng, P. Sun, C.H. Huang, J. Niu, X. Zhou, C.C. Crittenden, Perfluorooctanoic acid degradation using UV-Persulfate process: modeling of the degradation and chlorate formation, Environ. Sci. Technol. 50 (2015) 772–781.
[13] Z. Frontistis, E. Hapeshi, D. Fatta-Kassinos, D. Mantzavinos, Ultraviolet activated persulfate oxidation of methyl orange: a comparison between artificial neural networks and factorial design for process modelling, Photochem. Photobiol. Sci. 14 (2015) 528–535.
[14] Y.Q. Gao, N.Y. Gao, Y. Deng, Y.Q. Yang, Y. Ma, Ultraviolet (UV) light-activated persulfate oxidation of sulfamethazine in water, Chem. Eng. J. 195–196 (2012) 248–253.
[15] A. Soubh, N. Mokhtarani, The post treatment of composting leachate with a combination of ozone and persulfate oxidation processes, RSC Adv. 6 (2016) 76113–76122.
[16] A.S. Abu, A.H. Abdul, A.M. Nordin, Optimization of stabilized leachate treatment using ozone/persulfate in the advanced oxidation process, Waste Manage. 33 (2013) 1434–1441.
[17] Z. Wei, F.A. Villamena, L.K. Weavers, Kinetics and mechanism of ultrasonic activation of persulfate: an in situ EPR spin trapping study, Environ. Sci. Technol. 51 (2017) 3410–3417.
[18] B. Darsinou, Z. Frontistis, M. Antonopoulou, I. Konstantinou, D. Mantzavinos, Sono-activated persulfate oxidation of bisphenol A: kinetics, pathways and the controversial role of temperature, Chem. Eng. J. 280 (2015) 623–633.
[19] Q. Yang, Y. Zhong, H. Zhong, X. Li, W. Du, X. Li, R. Chen, G. Zeng, A novel pretreatment process of mature landfill leachate with ultrasonic activated persulfate: optimization using integrated taguchi method and response surface methodology, Process Saf. Environ. 98 (2015) 268–275.
[20] M.C. Cui, M. Jang, S.B. Lee, J. Khim, Sonochemical oxidation of cyanide using potassium peroxydisulfate as an oxidizing agent, Jpn. J. Appl. Phys. 51 (2012) 07GD13.
[21] S. Yang, P. Wang, X. Yang, G. Wei, W. Zhang, L. Shan, A novel advanced oxidation process to degrade organic pollutants in wastewater: microwave activated persulfate oxidation, J. Environ. Sci. 21 (2009) 1175–1180.
[22] J. Deng, Y. Shao, N. Gao, Y. Deng, C. Tan, S. Zhou, Zero-valent iron/persulate (Fe^0/PS) oxidation acetaminophen in water, Int. J. Environ. Sci. Technol. 11 (2014) 881–890.
[23] I. Hussain, Y. Zhang, S. Huang, X. Du, Degradation of p-chloroaniline by persulfate activated with zero-valent iron, Chem. Eng. J. 203 (2012) 269–276.
[24] Z. Aksu, Determination of the equilibrium, kinetic and thermodynamic parameters of the batch biosorption of nickel ions onto *Chlorella vulgaris*, Process Biochem. 38 (2002) 89–99.
[25] N. Brauner, M. Shacham, Statistical analysis of linear and nonlinear correlation of the Arrhenius equation constants, Chem. Eng. Process. 36 (1997) 243–249.
[26] N. Sahiner, H. Ozay, O. Ozay, N. Aktas, New catalytic route: hydrogels as templates and reactors for in situ Ni nanoparticle synthesis and usage in the reduction of 2- and 4-nitrophenols, Appl. Catal., A 385 (2010) 201–207.
[27] Y. Son, M. Lim, M. Ashokkumar, J. Khim, Geometric optimization of sonoreactors for the enhancement of sonochemical activity, J. Phys. Chem. C. 115 (2011) 4096–4103.
[28] P.R. Gogate, V.S. Sutkar, A.B. Pandit, Sonochemical reactors: important design and scale up considerations with a special emphasis on heterogeneous systems, Chem. Eng. J. 166 (2011) 1066–1082.
[29] D.V. Pinjari, A.B. Pandit, Cavitation milling of natural cellulose to nanofibrils, Ultrason. Sonochem. 17 (2010) 845–852.
[30] V.K. Saharan, M.P. Badve, A.B. Pandit, Degradation of reactive red 120 dye using hydrodynamic cavitation, Chem. Eng. J. 178 (2011) 100–107.
[31] Y.T. Shah, A.B. Pandit, V.S. Moholkar, Cavitation Reaction Engineering, Kluwer Academic/Plenum Publishers, New York, 1999.
[32] G.V. Buxton, W.P. Helman, A.B. Ross, Critical review of rate constants for reactions of hydrated electrons hydrogne atoms and hydroxyl radicals in aqueous solution, J. Phys. Chem. Ref. Data. 17 (1988) 513–886.
[33] I. Rykowska, W. Wasiak, Properties, threats, and methods of analysis of bisphenol A and its derivatives, Acta Chromatogr. 16 (2006) 7–27.
[34] C. Liang, C.J. Bruell, M. Marley, K. Sperry, Persulfate oxidation for in situ remediation of TCE. I. Activated by ferrous ion with and without a persulfate-thiosulfate redo couple, Chemosphere 55 (2004) 1213–1223.
[35] D.B. Thakur, R.M. Tiggelaar, Y. Weber, J.G.E. Gardeniers, L. Lefferts, K. Seshan, Ruthenium catalyst on carbon nanofiber support layers for use in silicon-based structured microreactors. Part II: Catalytic reduction of bromate contaminants in aqueous phase, Appl. Catal., B 102 (2011) 243–250.
[36] G.R. Peyton, The free-radical chemistry of persulfate-based total organic carbon analyzers, Mar. Chem. 41 (1993) 91–103.
[37] X.R. Xu, X.Z. Li, Degradation of azo dye orange G in aqueous solutions by persulfate with ferrous ion, Sep. Purif. Technol. 72 (2010) 105–111.
[38] A. Ghauch, A.M. Tuqan, Oxidation of bisoprolol in heated persulfate/H_2O systems: kinetics and products, Chem. Eng. J. 183 (2012) 162–171.
[39] Department of Chemistry – Florida State University, Activation Energy, https://www.chem.fsu.edu/chemlab/chm1046course/activation.html 1999, (accessed 13

January 2017).
[40] M. Cui, J. Choi, Y. Lee, J. Ma, D. Kim, J. Choi, M. Jang, J. Khim, Significant enhancement of bromate removal in drinking water: Implications for the mechanism of sonocatalytic reduction, Chem. Eng. J. 317 (2017) 404–412.
[41] J. Criquet, N.K.V. Leitner, Degradation of acetic acid with sulfate radical generated by persulfate ions photolysis, Chemosphere 77 (2009) 194–200.
[42] B. Venkatachalapathy, P. Ramamurthy, Reactions of nitrate radical with amino acids in acidic aqueous medium: a flash photolysis investigation, J. Photochem. Photobiol., A 93 (1996) 1–5.
[43] M. Exner, H. Herrmann, R. Zellner, Laser-based studies of reactions of the nitrateradical in aqueous solution, Ber. Bunsen Ges. 96 (1992) 470–477.
[44] P. Neta, R.E. Huie, A.B. Ross, Rate constants for reactions for inorganic radicals in aqueous solution, J. Phys. Chem. Ref. Data 17 (1988) 1027–1247.
[45] G.V. Buxton, M. Bydder, G.A. Salmon, J.E. Williams, The reactivity of chlorine atoms in aqueous solutions. Part III. The reaction of Cl• with solutes, Phys. Chem. Chem. Phys. 2 (2000) 237–245.
[46] O.P. Chawla, R.W. Fewenden, Electron spin resonance and pulse radiolysis studies of some reactions of SO4-l,2, J. Phys. Chem.-US 79 (1975) 2693–2700.
[47] X.Y. Yu, Z.C. Bao, J.R. Barker, Free radical reactions involving Cl•, Cl_2 ˙•, and SO_4 ˙• in the 248 nm photolysis of aqueous solutions containing S_2O_8 $^{2-}$ and Cl, J. Phys. Chem. A. 108 (2009) 295–308.
[48] M. Molkenthin, T. Tugba Olmez-Hanci, M.R. Jekel, I. Arslan-Alaton, Photo-Fenton-like treatment of BPA: effect of UV light source and water matrix on toxicity and transformation products, Water Res. 47 (2013) 5052–5064.
[49] F.J. Beltrán, F.J. Rivas, R. Montero-de-Espinosa, Ozone-enhanced oxidation of oxalic acid in water with cobalt catalysts. 2. Heterogeneous catalytic ozonation, Ind. Eng. Chem. Res. 42 (2003) 3218–3224.
[50] J. Sharma, I.M. Mishra, D.D. Dionysiou, V. Kumar, Oxidative removal of Bisphenol A by UV-C/peroxymonosulfate (PMS): kinetics, influence of coexisting chemicals and degradation pathway, Chem. Eng. J. 276 (2015) 193–204.
[51] Y. Son, Simple design strategy for bath-type high-frequency sonoreactors, Chem. Eng. J. 328 (2017) 654–664.
[52] A.O. Kondrakov, A.N. Ignatev, F.H. Frimmel, S. Brase, H. Horn, A.I. Revelsky, Formation of genotoxic quinines during bisphenol A degradation by TiO_2 photocatalysis and UV photolysis: a comparative study, Appl. Catal., B 160–161 (2014) 106–114.
[53] S. Fukahori, H. Ichiura, T. Kitaoka, H. Tanaka, Cpturing of bispheonol A photodecomposition intermediates by composite TiO_2-zeolite sheets, Appl. Catal., B 46 (2003) 453–462.
[54] Y. Wang, C.S. Hong, TiO_2 mediated photomineralization of 2-chlorobiphenyl: the role of O_2, Water Res. 34 (2000) 2791–2797.
[55] F. Minisci, A. Citterio, C. Giordano, Electron-transfer processes: peroxydisulfate, a useful and versatile reagent in organic chemistry, Acc. Chem. Res. 16 (1983) 27–32.
[56] J.R. Bolton, K.G. Bircger, W. Tumas, C.A. Tolman, Figure-of merit for the technical development and application of advanced oxidation technologies for both electric and solar-derived systems, Pure Appl. Chem. 73 (2001) 627–637.
[57] U.S. Energy Information Administration, Electricity, https://www.eia.gov/electricity/, 2017 (accessed 3 December 2017).
[58] Shanghai Tianli Chemical Co. Ltd., Sodium Persulfate 99% min, https://www.alibaba.com/product-detail/Sodium-Persulfate-99-min_60313285957.html?spm=a2700.7724857.main07.81.41993352srEcNi, 2017 (accessed 3 December 2017).